

MEMORY FORMATION

Diversity in neural firing dynamics supports both rigid and learned hippocampal sequences

Andres D. Grosmark^{1,2} and György Buzsáki^{2,3*}

Cell assembly sequences during learning are “replayed” during hippocampal ripples and contribute to the consolidation of episodic memories. However, neuronal sequences may also reflect preexisting dynamics. We report that sequences of place-cell firing in a novel environment are formed from a combination of the contributions of a rigid, predominantly fast-firing subset of pyramidal neurons with low spatial specificity and limited change across sleep-experience-sleep and a slow-firing plastic subset. Slow-firing cells, rather than fast-firing cells, gained high place specificity during exploration, elevated their association with ripples, and showed increased bursting and temporal coactivation during postexperience sleep. Thus, slow- and fast-firing neurons, although forming a continuous distribution, have different coding and plastic properties.

The restructuring of hippocampal networks through synaptic plasticity is necessary for the formation of new episodic memories. Replay of hippocampal place-cell (1) sequences during sharp wave ripples (SPW-Rs) of waking immobility (2–5) and non-rapid eye movement sleep (6–13) after learning has been proposed to support memory consolidation (10–13). Replay is conceptualized and typically studied as a phenomenon with higher-order interactions within populations of neurons taken to have similar properties (10, 14). However, networks built from similar neurons are unstable (15), and recent findings demonstrate that biophysical properties of cortical pyramidal neurons are highly diverse and characterized by lognormal distributions of synaptic weights, long-term firing rates, and spike bursts (16). Furthermore, temporal correlations of hippocampal neurons are largely preserved across brain states and environmental situations, suggesting that learning-induced changes are constrained within a dynamically stable network (16, 17). An example of a preexisting bias between place-cell sequences in a novel environment and sleep before the novel experience (preplay) has been described (18–20), although its computational relevance has been questioned recently (14). To clarify the relationship between preexisting biophysical properties of neurons and their contribution to learning, characterization of individual neurons is necessary. We performed such analyses during sleep in rats before and after they explored a novel environment.

Simultaneous recordings of well-isolated CA1 pyramidal single units were performed in four rats. Several methods were used to assess the relationship between firing patterns during explo-

ration of one of two linear or a circular track (MAZE) in rooms B, C and D, respectively, and candidate SPW-R sequences during preexperience sleep (PRE) and postexperience sleep (POST) in the home cage in room A (fig. S1) (21). First, a spatial Bayesian decoder (2), constructed from the firing-rate vectors of place cells ($n = 491$ cells) during track running (eight novel exploration sessions), was applied to all candidate ripple events (21) (figs. S2 to S4) of PRE, MAZE, and POST immobility epochs to estimate the posterior probabilities of position in forward (2, 5, 9) or reverse virtual traversals of the track (3, 4) (Fig. 1, A and B). These virtual traversals were measured as weighted correlations over the Bayesian derived posteriors for place across all 20-ms bins in each ripple event (21) and normalized as Z scores [rZ (sequence score) (21)] (figs. S5 to S8).

To determine each place cell's contribution to PRE and POST sequences [per cell contribution (PCC)], a PCC score was defined as the neuron's mean contribution across all PRE and POST putative events as determined by a cell-specific shuffling technique (21). Neurons that showed significant PCC scores in either PRE or POST were considered to be strongly contributing to sequence formation ($n = 216$ neurons (Fig. 2B) (21). Importantly, the majority of neurons strongly contributing to PRE (73%) also contributed to POST sequences (Fig. 2C and fig. S19), suggesting that these neurons represent rigid network elements. Strongly contributing neurons < 50 percentile of that session's PRE to POST sleep PCC change (ΔPCC) were classified as rigid cells (blue x's in Fig. 2B), whereas those > 50 percentile as plastic cells (red x's in Fig. 2A and figs. S9 to 11). Rigid and plastic neurons were similarly distributed along the track (fig. S2). The contribution of individual neurons to the overall population $\Delta POST$ -PRE score ($POST\ rZ - PRE\ rZ$) was assessed by either shuffling or excluding neurons with increasing or decreasing ΔPCC scores from the analysis (Fig. 2C and fig. S12) (21). Replay ($POST > PRE$)

was eliminated after shuffling or removal of the top 10 to 20% of cells with the highest ΔPCC scores, whereas it remained after shuffling or removal of the bottom 75% (Figs. 2, C and D, and fig. S12). These results suggest that from the PRE to the POST sleep, plastic neurons are added to a pre-existing backbone structure, leading to an increase in maze-related sequential activity (replay) associated with learning (Fig. 2C).

Although both rigid and plastic neurons contributed to replay sequences, the nature of their representation was different. Plastic neurons had higher place-specific indices and fewer place fields compared with rigid cells (Fig. 3A), and plastic but not rigid neurons increased their spatial specificity steadily during learning (Fig. 3B and fig. S13). Neither overall firing-rate changes (figs. S14 and S15) nor potential errors in neuronal clustering or neuron classification (figs. S2 and S11) could account for the above differences. These findings suggest that precision in spatial coding is a property developed during maze running by a small plastic subset of cells.

Next, we asked whether rigid and plastic neurons have different biophysical and network properties. Session-wide firing rates of rigid neurons were significantly higher compared with plastic neurons (Fig. 4, A and B, and figs. S14 and S15). Ripple-related spiking, bursting, and pair-wise coactivation were higher in plastic versus rigid neurons (Fig. 4A and figs. S14 to S16). In PRE sleep, coactivity was dominated by fast-firing neurons, and these correlations remained unchanged into POST sleep. In contrast, slow-firing neurons showed the strongest increases in coactivation from PRE to POST sleep (Fig. 4B). Pair-wise coactivity and temporal bias patterns were stable from PRE to POST for pairs of rigid cells, whereas plastic cell pair interactions were modified by experience on the novel maze (10) (figs. S16 and S17).

Because the above analyses indicated that overall firing rates and ripple-related activity of neurons predicted their coding and plastic features, in our final analysis we divided place cells into equal subgroups by either “off-line” sleep-firing rate or ripple-rate gain and repeated the Bayesian place decoding analysis for each group. Low-rate neurons (median, 0.39 Hz) contributed more spatial information per spike on the maze and displayed increased within-ripple firing-rate gains from PRE to POST sleep than high-rate cells (median, 1.12 Hz) (fig. S16). Slow-firing, but not fast-firing, neurons increased their contribution to neuronal sequences from PRE to POST sleep (Fig. 4D). Conversely, PRE to POST increases in sequence content were limited to cells that showed a high degree of ripple-specific recruitment (gain) (Fig. 4E and figs. S20 to S22), suggesting that ripples are privileged windows for learning-related changes in excitability. Similar results were obtained using several Bayesian and non-Bayesian replay methods (figs. S19 to S22).

Using several established and newly developed methods, we demonstrate that sequences of place cells in a novel environment are formed from a combination of relatively fast-firing group of pyramidal neurons with relatively unchanging temporal dynamics and a slow-firing plastic subset of

¹Department of Neuroscience, Columbia University Medical Center, New York, NY 10019, USA. ²The Neuroscience Institute, School of Medicine, New York University, New York, NY 10016, USA. ³Center for Neural Science, New York University, New York, NY 10016, USA.

*Corresponding author. E-mail: gyorgy.buzsaki@nyumc.org

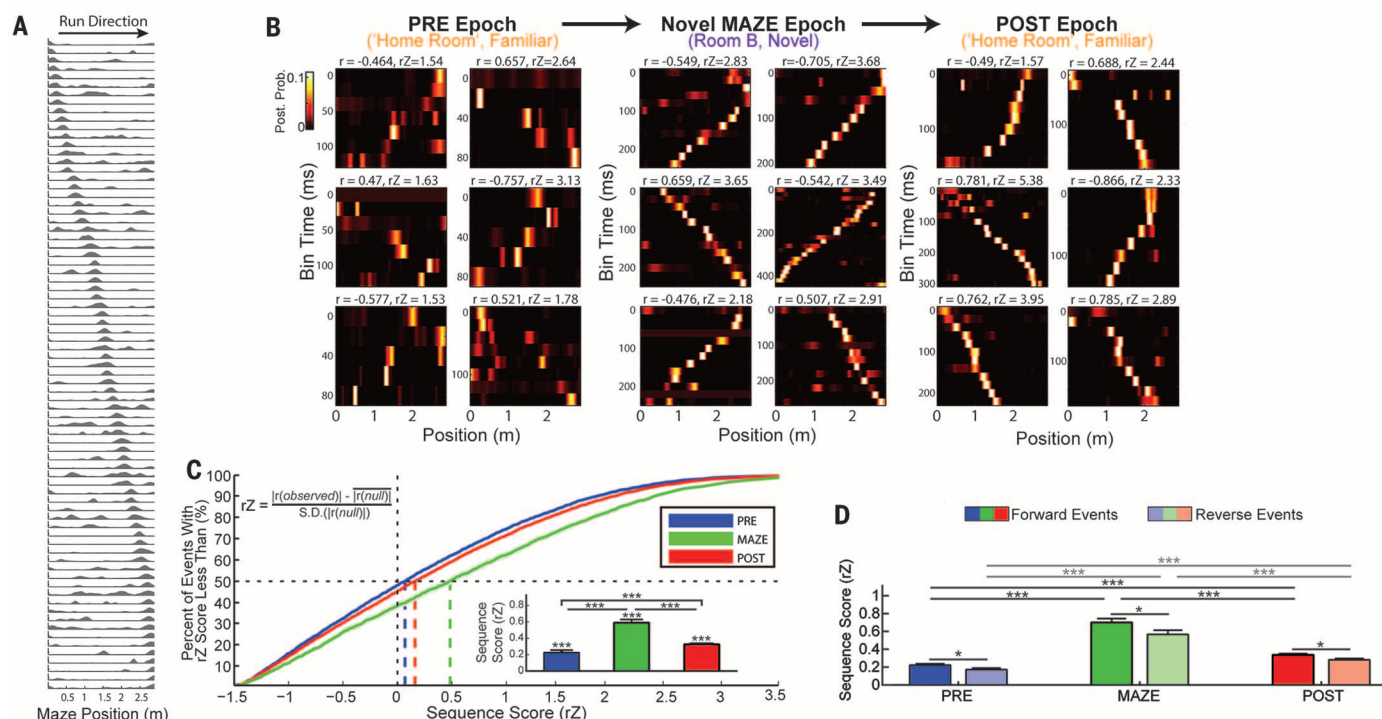


Fig. 1. PRE and POST maze sequence events. (A) Simultaneous recording of 77 place cells (rightward runs) used to generate a sequence template. (B) Representative forward and reverse sequences during PRE maze sleep, immobility in the novel MAZE, and POST-learning sleep. (C) Cumulative distribution of rZ for PRE, MAZE, and POST events, and 95% confidence intervals. Vertical dashed lines, medians. Inset, mean \pm SE of sequence scores in each condition. $*P < 0.05$; $**P < 0.005$; $***P < 0.0005$ (Kruskal-Wallis test, followed by post hoc Tukey-Kramer tests). Sign-rank tests were used for within-condition significance testing. (D) As inset in (C), but events with forward and reverse sequences are shown separately (within epoch comparisons, ranked-sum test).

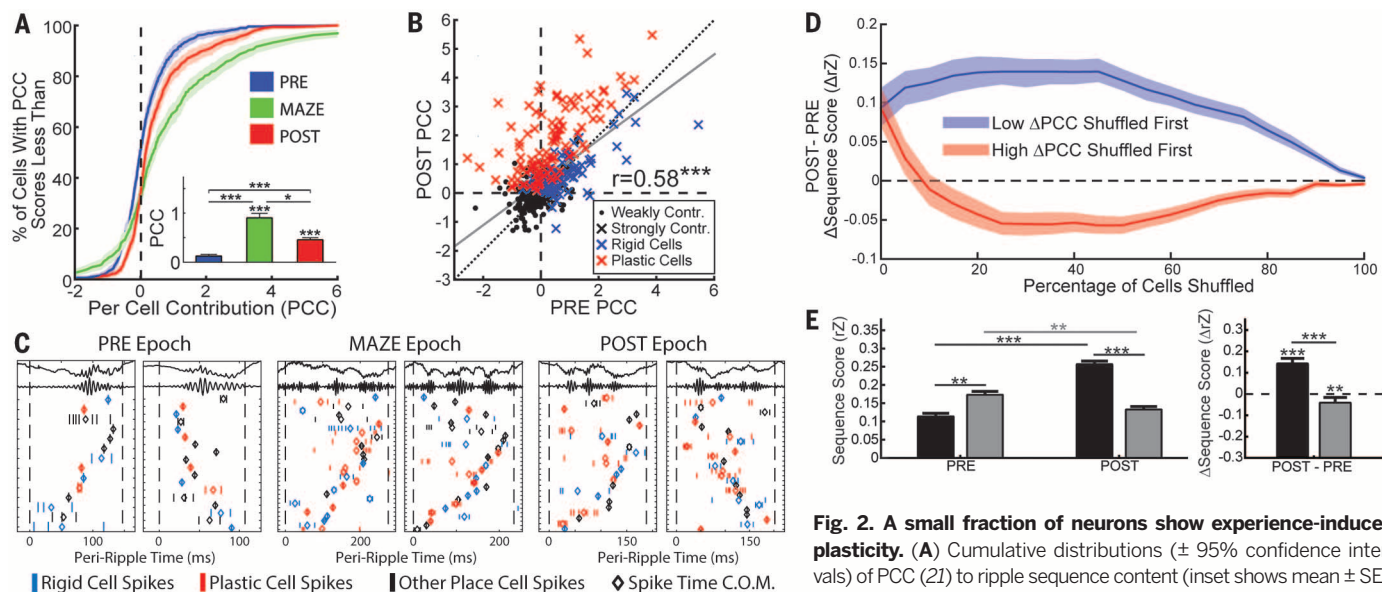


Fig. 2. A small fraction of neurons show experience-induced plasticity. (A) Cumulative distributions (\pm 95% confidence intervals) of PCC (2I) to ripple sequence content (inset shows mean \pm SE). (B) Relationship between each neuron's contribution to PRE and POST PCC scores. Neurons strongly contributing to either PRE or POST (2I) are marked with X; others are marked with dots. Strongly contributing neurons in the lower 50th percentile of that session's PRE versus POST change (Δ PCC) were considered rigid cells and those in the upper 50th percentile as plastic cells. (C) Raster and local field potential (LFP) plots of example ripple events from the PRE, MAZE, and POST epochs (diamonds show within-ripple spike-time center of mass). These six events correspond to the top row of Fig. 1B. Rigid and plastic cell spikes are shown in blue and red, respectively. Although rigid cells tend to predominate in the PRE epoch, the marked increase in sequence content observed in the MAZE and POST epochs is driven by the recruitment of plastic cells. (D) To assess the contribution of neurons with differing Δ PCC scores to the change in virtual travel content from the PRE to the POST epoch, the replay analysis was repeated using templates in which an increasing percentage (x axis) of neuron's place fields were shuffled either beginning with those that showed the lowest Δ PCC values (blue line) (shaded area shows bootstrapped 95% confidence interval) or beginning with neurons with the highest Δ PCC scores (red line). (E) Effect on sequence content of removal of rigid (black) or plastic (gray) neurons. The PRE to POST increase in sequence content is attributable to only a small number of plastic cells.

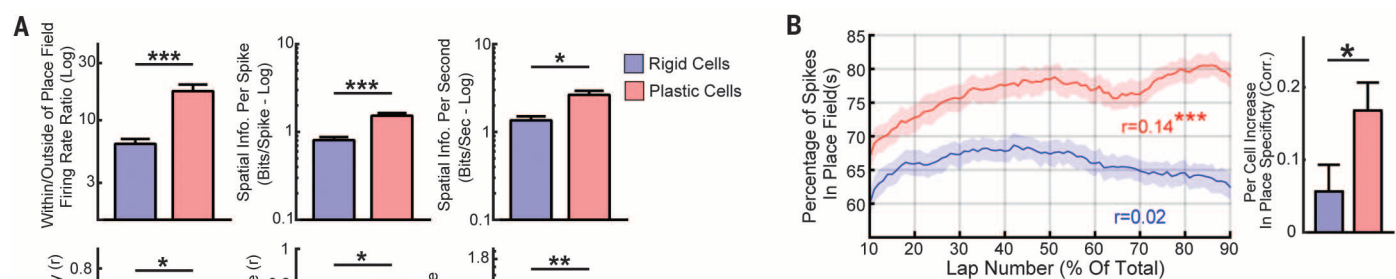


Fig. 3. Properties of rigid and plastic neurons differ on the novel maze. (A) Differences in spatial coding properties (top panels, log-mean \pm log-SE; bottom panels, mean \pm SE, rank-sum tests). (B) Within-session improvement of plastic neurons' in-field versus outside field firing ratios. Plastic cells improved spatial coding overlaps on the maze; left panel shows the within-session changes of place field representation changes (mean \pm SE) (21).

for rigid (blue) or plastic (red) neurons (shaded region shows bootstrapped 95% confidence interval). Right panel, per cell summary of within-field firing specificity changes (mean \pm SE) (21).

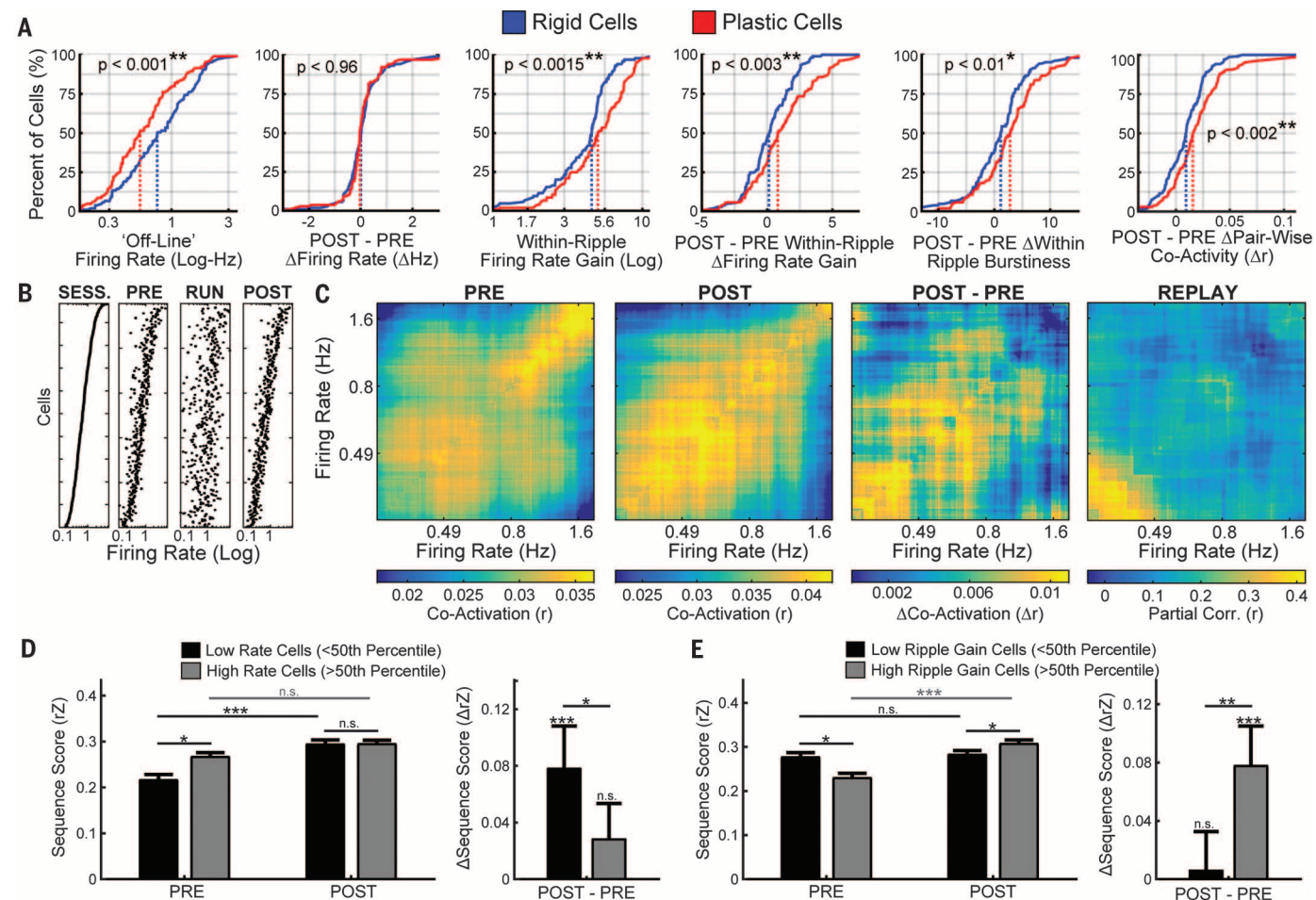


Fig. 4. Low-firing-rate, high-ripple-recruitment neurons show high learning-related plasticity. (A) Summary of excitability and synchrony profiles of rigid and plastic cells. Each panel shows the cumulative distributions of the two groups; dashed lines show medians (P values, rank-sum tests). (B) To examine the relationship between firing rates and learning-related changes in pair-wise coactivation (Pearson's correlation of firing rates in 100-ms bins), neurons in PRE, MAZE, and POST were sorted by their overall session (SESS) firing rates [(B), left panel]. (C) Coactivation was assessed across overlapping groups each containing 20% of place cells with similar firing rates (step size,

1% of cells). Although fast-firing cells dominated the coactivation structure during the PRE (left panel), it was the slow-firing cells that showed the highest increase in coactivation from PRE to POST (middle two panels). Moreover, it was the slow-firing cells that showed the greatest replay (partial correlation across coactivation values between RUN and POST, accounting for PRE). (D and E) An additional replay analysis restricted to place cells with either low or high firing rates (D) or within-ripple firing-rate gains [(E), annotation same as in Fig. 2D] confirms the findings obtained using the PCC method.

neurons (22). Firing properties of neurons predicted their rigid (18, 19) and plastic (10) features. Slow-firing neurons gained high place specificity during maze exploration (23, 24) and showed increased ripple-related recruitment during POST-experience sleep. In contrast, fast-firing neurons had low selectivity (16, 25), have been shown previously to project to multiple targets (26) and to form an interactive subnetwork responsible for global stability, thus allowing plasticity to take place in the remaining majority of slow-firing cells (16, 17). Fast-firing neurons may generalize across situations, whereas slow-firing neurons may differentiate among them (27). Because replay sequence-forming neurons are drawn from the wide span of a continuous log-rate distribution (16) with varying coding, biophysical, circuit, and plasticity properties, these events can forward a synthesis of preexisting and new information to downstream observer neurons.

REFERENCES AND NOTES

1. J. O'Keefe, L. Nadel, *The Hippocampus as a Cognitive Map* (Oxford Univ. Press, 1978).
2. T. J. Davidson, F. Kloosterman, M. A. Wilson, *Neuron* **63**, 497–507 (2009).
3. K. Diba, G. Buzsáki, *Nat. Neurosci.* **10**, 1241–1242 (2007).
4. D. J. Foster, M. A. Wilson, *Nature* **440**, 680–683 (2006).
5. B. E. Pfeiffer, D. J. Foster, *Nature* **497**, 74–79 (2013).
6. D. Dupret, J. O'Neill, B. Pleydell-Bouverie, J. Csicsvari, *Nat. Neurosci.* **13**, 995–1002 (2010).
7. G. Girardeau, K. Benchenane, S. I. Wiener, G. Buzsáki, M. B. Zugaro, *Nat. Neurosci.* **12**, 1222–1223 (2009).
8. H. S. Kudrimoti, C. A. Barnes, B. L. McNaughton, *J. Neurosci.* **19**, 4090–4101 (1999).
9. A. K. Lee, M. A. Wilson, *Neuron* **36**, 1183–1194 (2002).
10. M. A. Wilson, B. L. McNaughton, *Science* **265**, 676–679 (1994).
11. G. Buzsáki, *Neuroscience* **31**, 551–570 (1989).
12. M. E. Hasselmo, *Trends Cogn. Sci.* **3**, 351–359 (1999).
13. G. Buzsáki, *Hippocampus* **25**, 1073–1188 (2015).
14. D. Silva, T. Feng, D. J. Foster, *Nat. Neurosci.* **18**, 1772–1779 (2015).
15. W. Gerstner, W. M. Kistler, R. Naud, L. Paninski, *Neuronal Dynamics: From Single Neurons to Networks and Models of Cognition* (Cambridge Univ. Press, 2014).
16. K. Mizuseki, G. Buzsáki, *Cell Rep.* **4**, 1010–1021 (2013).
17. D. A. Panatier, B. L. McNaughton, *Science* **345**, 8480–8492 (2015).
18. G. Dragoi, S. Tonegawa, *Nature* **469**, 397–401 (2011).
19. G. Dragoi, S. Tonegawa, *Proc. Natl. Acad. Sci. U.S.A.* **110**, 9100–9105 (2013).
20. H. F. Ólafsdóttir, C. Barry, A. B. Saleem, D. Hassabis, H. J. Spiers, *eLife* **4**, e06063 (2015).
21. Materials and methods are available as supplementary materials on Science Online.
22. G. Dragoi, K. D. Harris, G. Buzsáki, *Neuron* **39**, 843–853 (2003).
23. K. C. Bittner et al., *Nat. Neurosci.* **18**, 1133–1142 (2015).
24. S. Cheng, L. M. Frank, *Neuron* **57**, 303–313 (2008).
25. P. D. Rich, H.-P. Liaw, A. K. Lee, *Science* **345**, 814–817 (2014).
26. S. Cioocchi, J. Passecker, H. Malagon-Vina, N. Mikus, T. Klausberger, *Science* **348**, 560–563 (2015).
27. G. Buzsáki, *Science* **347**, 612–613 (2015).

ACKNOWLEDGMENTS

This work was supported by NIH grants NS075015, MH54671, and MH102840; the Simons Foundation; and the G. Harold and Leila Y. Mathers Foundation. We thank J. Long for invaluable experimental support and B. Watson, S. McKenzie, L. Roux, and S. Tuncdemir for discussion and advice. Spike and LFP data are available at CRCNS.org.

SUPPLEMENTARY MATERIALS

www.sciencemag.org/content/351/6280/1440/suppl/DC1
Materials and Methods
Figs. S1 to S22
References (28–36)

6 August 2015; accepted 11 February 2016
10.1126/science.aad1935

NEURODEVELOPMENT

Sequential transcriptional waves direct the differentiation of newborn neurons in the mouse neocortex

Ludovic Telley,^{1,7*} Subashika Govindan,^{1,7*} Julien Prados,^{1,7}
Isabelle Stevant,^{2,7} Serge Nef,^{2,7} Emmanouil Dermitzakis,^{2,5,6,7}
Alexandre Dayer,^{1,3,7} Denis Jabaudon^{1,4,7†}

During corticogenesis, excitatory neurons are born from progenitors located in the ventricular zone (VZ), from where they migrate to assemble into circuits. How neuronal identity is dynamically specified upon progenitor division is unknown. Here, we study this process using a high-temporal-resolution technology allowing fluorescent tagging of isochronic cohorts of newborn VZ cells. By combining this *in vivo* approach with single-cell transcriptomics in mice, we identify and functionally characterize neuron-specific primordial transcriptional programs as they dynamically unfold. Our results reveal early transcriptional waves that instruct the sequence and pace of neuronal differentiation events, guiding newborn neurons toward their final fate, and contribute to a road map for the reverse engineering of specific classes of cortical neurons from undifferentiated cells.

During neocortical development, distinct classes of neurons assemble to form local and long-range circuits. Although class-specific genes and features identify cortical neuron types relatively late in differentiation (1–5), early postmitotic fate specification programs have been inaccessible. Here, we describe the dynamic transcriptional activity controlling layer 4 (L4) excitatory neuron birth and differentiation in the mouse neocortex.

Mammalian cortical progenitor cells in the ventricular zone (VZ) undergo DNA synthesis [S-phase, susceptible to bromodeoxyuridine (BrdU) labeling] at the basal border of the VZ and mitosis (M-phase, lasting about an hour at midcorticogenesis in mice) when their soma is apically located, adjacent to the ventricular space (6, 7). At this location, mitotic cells are susceptible to labeling by intraventricular injection of carboxy-fluorescein esters ["FlashTag" (FT)], which bind to and fluorescently label intracellular proteins (8). The short extracellular half-life of FT in the mouse ventricular space ensures effective pulse-labeling of juxtaventricular dividing cells (Fig. 1A and fig. S1). Intracellularly, FT is linearly diluted at each mitosis, such that fluorescence reflects the number of cell divisions that have occurred since the time of labeling (fig. S1,

D and E, and movie S1) (8). FT⁺ newborn cells synchronously moved away from the ventricular wall within 3 hours of labeling (Fig. 1A, bottom), reached the subventricular zone (SVZ) within 12 hours, and entered the cortical plate (CP) 24 to 48 hours after mitosis (Fig. 1B). Isochronic cohorts of VZ cells born at the time of injection can thus be specifically identified and tracked during their initial differentiation.

The laminar fate of FT⁺ neurons was linked to the day of FT injection at all ages examined [embryonic day (E) 11.5 to 17.5] (fig. S2 and Fig. 1C). At postnatal day (P) 7, when neuronal migration is complete, E14.5-labeled FT⁺ neurons were restricted to a sublamina of L4 (Fig. 1C). These neurons were born at the time of the FT pulse, not later, because they mostly remained unlabeled after continuous BrdU administration beginning at the time of the FT pulse (fig. S1, B to D). Injection of FT at E14 and E14.5 using two dye colors in the same embryo showed two distinct populations of labeled neurons within L4 at P7, revealing a tight relationship between time of birth and final radial location, even within a single layer (Fig. 1D). Thus, we used E14.5 FT injections to label L4 neurons *in vivo* from the time of mitosis in the VZ and track their early molecular differentiation.

We observed that newborn cells sequentially expressed PAX6, a VZ marker, TBR2 a SVZ marker, and the early neuronal protein TBR1 (9, 10) within the first 48 hours after mitosis (fig. S3). This reveals a highly dynamic cellular process characterized by overlapping signature shifts in protein expression. For an unbiased account of the transcriptional programs active just after cell birth in single cells, we isolated E14.5-born FT⁺ cells 6, 12, 24, and 48 hours after mitosis by using cortical microdissection followed by fluorescence-activated cell sorting

¹Department of Basic Neurosciences, University of Geneva, Switzerland. ²Department of Genetic Medicine and Development, University of Geneva, Switzerland.

³Department of Psychiatry, Geneva University Hospital, Switzerland. ⁴Clinic of Neurology, Geneva University Hospital, Switzerland. ⁵Biomedical Research Foundation Academy of Athens, Greece. ⁶Center of Excellence in Genomic Medicine Research, King Abdulaziz University, Saudi Arabia. ⁷Institute for Genetics and Genomics in Geneva (iG3), University of Geneva, Switzerland.

*These authors contributed equally to this work. †Corresponding author. E-mail: denis.jabaudon@unige.ch

Diversity in neural firing dynamics supports both rigid and learned hippocampal sequences

Andres D. Grosmark and György Buzsáki

Science **351** (6280), 1440-1443.
DOI: 10.1126/science.aad1935

Coding what is known and what is new

Do neural activity patterns during sleep reflect the replay of a novel experience or an invariant preexisting dynamic? Grosmark and Buzsáki observed that both familiar and novel aspects of learned information are replayed during synchronous bursts of activity in the hippocampus. Familiarity was encoded by fast-firing less-modifiable neurons that showed rate and sequence correlations that persisted into postlearning sleep. The novel features of an experience were represented by a different set of slowly firing and highly plastic cells.

Science, this issue p. 1440

ARTICLE TOOLS

<http://science.sciencemag.org/content/351/6280/1440>

SUPPLEMENTARY MATERIALS

<http://science.sciencemag.org/content/suppl/2016/03/23/351.6280.1440.DC1>

REFERENCES

This article cites 33 articles, 9 of which you can access for free
<http://science.sciencemag.org/content/351/6280/1440#BIBL>

PERMISSIONS

<http://www.sciencemag.org/help/reprints-and-permissions>

Use of this article is subject to the [Terms of Service](#)